

Periodic electric-field domains in optically excited multiple-quantum-well structures

M. Ryzhii and V. Ryzhii*

Computer Solid State Physics Laboratory, University of Aizu, Aizu-Wakamatsu 965-8580, Japan

R. Suris

A.F. Ioffe Physical-Technical Institute RAS, St. Petersburg 194021, Russia

C. Hamaguchi

Department of Electronic Engineering, Osaka University, Suita, Osaka 565-0871, Japan

(Received 30 August 1999)

We demonstrate using an ensemble Monte Carlo particle modeling that periodic electric-field domains can arise in optically excited multiple quantum well structures under applied voltage. In particular, the formation of the electric-field distributions with the period equal to twice the structure period is possible. This effect is attributed to the excitation of the recharging waves due to decreasing energy dependence of the capture rate of hot electron capture into quantum wells and nonlocal heating of electrons by electric field.

I. INTRODUCTION

Electron (hole) phenomena in semiconductor superlattices have been the topic of extensive experimental and theoretical studies for almost thirty years starting from the papers by Esaki and Tsu.^{1,2} Electron transport phenomena in superlattices and their device application have been extensively studied.³⁻⁹ A great deal of attention has also been paid to the electron transport and capture effects in multiple quantum well (QW) structures with a weak coupling between QW's. This, in part, is due to the use of such QW structures in infrared photodetectors utilizing intersubband transitions.¹⁰ Apart from thermo- or photo-stimulated bound-to-continuum transitions of electrons, the operation of QW infrared photodetectors (QWIP's) is associated with the electron vertical transport above the barriers and capture into QW's, as well as the injection of electrons from the emitter contact. Under the effect of applied electric field and photoexcitation by infrared radiation, the electron system in a QWIP is usually far from equilibrium. The diversity of effects determining the characteristics of QWIP's makes these devices very interesting from a physical point of view.

As reasoned previously,¹⁰⁻¹⁵ the electric-field distributions in QW structures in which the electron transport is associated with electrons in the continuum states are primarily monotonic. They correspond to rather smooth distributions of the potential. The combined effect of optical excitation and injection from the emitter usually results in the formation of the electric-field domain near the injecting contact (with either high- or low-electric field) with nearly uniform electric field in the structure bulk. The electric-field distributions of this type were invoked for the explanation of some features of multiple QW structures, in particular, the details of their current-intensity and current-voltage characteristics.¹⁴⁻¹⁶

In this paper, we study the response of multiple QW structures to steplike pulses of incident infrared radiation causing the photoionization of QW's due to the electron bound-to-continuum transitions. An ensemble Monte Carlo

(MC) particle method is used for this purpose. We show that the evolution of electric-field distributions in multiple QW structures can be fairly complex. It exhibits the excitation of the waves of QW recharging resulting in the formation of periodic electric-field and, hence, charge distributions in wide ranges of applied voltages and powers of infrared radiation. In particular, periodic electric-field domain structures can have the period equal to twice the QW structure period. In this case, odd-numbered QW's are positively charged while those with even indexes have negative charges.

II. MODEL

We consider *n*-type Al_{0.22}Ga_{0.78}As/GaAs multiple QW structures with thin narrow-gap doped layers (QW's) separated by relatively thick wide-gap undoped layers playing a role of the inter-QW barriers. The QW structures are supplied by contact regions made of a doped material of the same type as the material of QW's. Due to large thicknesses of the barriers, the tunneling of electrons between QW's is neglected, so that the vertical electron transport across the structure is associated with the propagation of electrons above the barriers. However, the electron injection from the emitter contact is due to tunneling through the top of the first (emitter) barrier in the structure stimulated by the electric field in this barrier. The tunneling results in the appearance of the injected electrons in the continuum states above the barriers. It is assumed that the energy of incident infrared photons $\hbar\Omega \geq \epsilon_i$, where ϵ_i is the ionization energy of QW's. We restrict ourselves by the exploration of QW structures optically excited by strong enough radiation, so that the photoionization of QW's dominates the thermionic emission from them.

The response of the QW structure under consideration to infrared pulses is associated with the following processes: (1) photoexcitation of electrons from the bound states in QW's into the continuum states, (2) propagation of mobile electrons across the QW structure, (3) capture of electrons and

their reflection from QW's, (4) tunneling injection of electrons from the emitter contact due to the increase of the electric field the first barrier caused by the redistribution of the electric potential as a consequence of the recharging of QW's, and (5) escape of electrons reached the collector contact. The heating of electrons in the continuum states leads to the change in electron energies and, hence, influences the electron transport and capture.

We describe the nonequilibrium electron system in QW structures in response to infrared radiation in the framework of an ensemble MC particle method. The usual MC method is adapted for peculiar features of the QW structures under consideration by the inclusion of the electron capture and photoionization processes. The self-consistent electric potential (field) obeys the Poisson equation which accounts for both the distributed charges of mobile electrons propagating above the barriers and localized charges of QW's:

$$\frac{d^2\varphi}{dx^2} = \frac{4\pi e}{\epsilon} \left[\sum_{n=1}^N (\Sigma_n - \Sigma_d) \delta(x-nL) + \rho - \rho_d \right], \quad (1)$$

where e is the electron charge, ϵ is the dielectric constant, Σ_n is the electron sheet concentration in the n th QW ($n = 1, 2, \dots, N$), N is the number of QW's in the structure, ρ is the concentration of electrons above the barriers, Σ_d and ρ_d are the donor sheet concentration in QW's and the donor concentration in the barriers, respectively, $L = L_w + L_b \approx L_b$ is the QW structure period, L_w and L_b are the thicknesses of the QW and the barrier, $\delta(x)$ is the QW form-factor, which is assumed to be similar to the Dirac δ function (due to $L_w \ll L_b \approx L$), and x is the coordinate in the direction perpendicular to the QW plane.

The boundary conditions have the following form:

$$\varphi|_{x=0} = 0 \quad \text{and} \quad \varphi|_{x=W} = V, \quad (2)$$

where $W = NL_w + (N+1)L_b$ is the net thickness of the QW structure and V is the applied bias voltage. The density of the injected current is given by

$$j = j_m \exp\left(-\frac{E_t}{E_e}\right). \quad (3)$$

Here, j_m is the maximum current density provided by the emitter contact, E_t is the characteristic tunneling field, and $E_e = E|_{x=0}$ is the electric field at the emitter contact. The rate of photoexcitation for the n th QW is given by the formula

$$G_n = \sigma \Sigma_n I, \quad (4)$$

where σ is the cross-section of the electron photoescape from a QW and I is the intensity of infrared radiation. The Poisson equation, similar in form to Eq. (1), with Eqs. (2) and (3) were used previously in both numerical^{12,13,17-19} and theoretical²⁰⁻²² studies of different effects in multiple QW structures.

The momentum distribution of the injected electrons is assumed to be corresponding to the tunneling nature of injection through a trapezoidal (under the effect of the electric field) emitter barrier. The collector contact absorbs all electrons passed the last barrier.

The MC model used for the calculations takes into account the features of the material band structures, and all

significant scattering mechanisms, including the electron reflection from the QW-barrier heterointerfaces. The capture of electrons (i.e., their transitions from the continuum states above the barriers into the bound states in QW's) is assumed to be associated primarily with the optical phonon emission.²³⁻²⁶ The interaction of mobile Γ electrons with QW's is described as their reflection, transmission, or capture. The ratio of the reflection and transmission probabilities is calculated quantum mechanically (in the Kane model framework) using the previously obtained formulas.²⁷ The transport of L and X electrons across the QW interfaces is considered classically. This approach suggests that semiclassical modeling of the capture processes may be sufficient, as was shown recently.²⁸ The MC method implemented in this paper is akin to that previously used by some of us for the calculations of the velocity-field relation and the macroscopic capture parameter in QW structures,¹⁷ as well as for the evaluation of their high-frequency performance.^{18,19}

The QW structure parameters used in the calculations are as follows: the number of QW's $N = 5, 6, 21$, and 50 , the QW structure period $L = 52$ nm ($L_w = 4$ nm and $L_b = 48$ nm), the barrier donor concentration $\rho_d = 10^{15}$ cm⁻³, the QW donor sheet concentration $\Sigma_d = 10^{12}$ cm⁻², the maximum emitter current density $j_m = 1.6 \times 10^6$ A/cm², and the emitter tunneling field $E_t = 340$ kV/cm. A structure with five QW's and significantly lower QW doping ($\Sigma_d = 2 \times 10^{11}$ cm⁻²) and a structure with 21 QW's having the period of $L = 34$ nm were also considered for comparison. The applied voltages V provided the average electric field $E = V/W = 5 - 30$ kV/cm. Such structure parameters correspond to the standard QW structures in QWIP's and the above range of the average electric fields is usual for these devices operation (see, for example, Ref. 10). The photoescape cross section, average initial energy of photoexcited electrons, and intensity of radiation were assumed to be $\sigma = 2 \times 10^{-15}$ cm², $\Delta = \hbar\Omega - \epsilon_i = 10$ meV, and $I = (10^{21} - 10^{24})$ cm⁻² s⁻¹, respectively.

III. RESULTS

We studied the response of QW structures with different parameters at different applied voltages to steplike pulses of infrared radiation. The initial states corresponded to nearly uniform electric-field distributions with neutral QW's.

Figure 1 shows the temporal transformation of the electric-field distribution in a QW structure with five QW's and $\Sigma_d = 10^{12}$ cm⁻² for the infrared photon flux of $I = 10^{23}$ cm⁻² s⁻¹. It follows from Fig. 1 that at the initial stage the electric-field is a monotonic function of the coordinate step-wisely decreasing in the direction from the injecting contact to the collector. The steps are associated with the depletion of QW's due to the photoescape of electrons when the injected current does not provide yet the required capture rates to compensate the loss of electrons by QW's. At later times the electric-field distribution becomes nonmonotonic, having in the beginning one minimum. Thereafter, the number of minima and maxima sequentially increases. The electric-field distribution stabilizes at around $t = 20$ ns. The electric-field distributions at different moments and, in particular, the final steady distribution correspond to both positive and negative charges of QW's. The temporal varia-

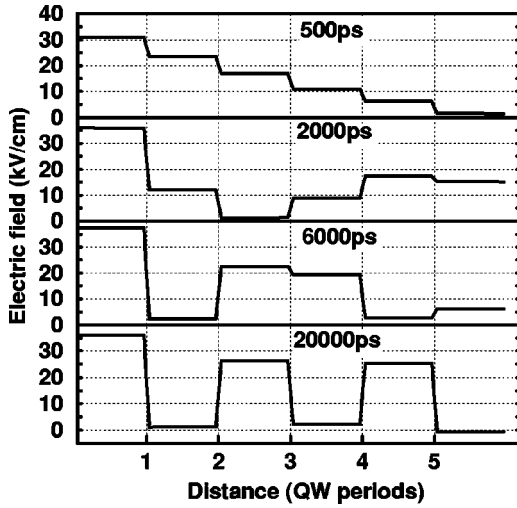


FIG. 1. Temporal transformation of spatial electric-field distribution in QW structure with five QW's at $E=15$ kV/cm and $I=10^{23}$ cm $^{-2}$ s $^{-1}$.

tions of electric fields in the barriers and electron sheet concentrations in QW's indicate the excitation of the recharging waves similar in nature to those in compensated semiconductors with traps.^{29–31} From the physical standpoint, the main distinction between recharging waves in structures with QW's and traps is associated with the spatial periodicity of QW locations and random distribution of traps. However, this distinction can lead to a pronounced difference in final stable states arisen as results of nonlinear transformations of the recharging waves. As seen in Fig. 1, the development recharging waves in QW structures can lead to stable periodic electric-field domain structures with the period λ equal twice of the QW structure period L and the amplitude damping in the direction from the emitter to collector contact. Such nearly periodic domains arise also in the same QW structure but under different average electric fields (bias voltages) and different infrared photon fluxes (see Fig.

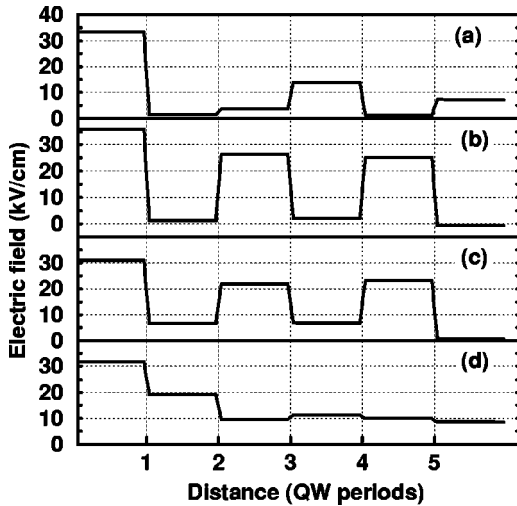


FIG. 2. Stable periodic electric-field domains in structure with five QW's for (a) $E=10$ kV/cm and $I=10^{23}$ cm $^{-2}$ s $^{-1}$, (b) $E=15$ kV/cm and $I=10^{23}$ cm $^{-2}$ s $^{-1}$, (c) $E=15$ kV/cm and $I=10^{22}$ cm $^{-2}$ s $^{-1}$, and (d) the same as for (b) but with $\Sigma_d=2 \times 10^{11}$ cm $^{-2}$.

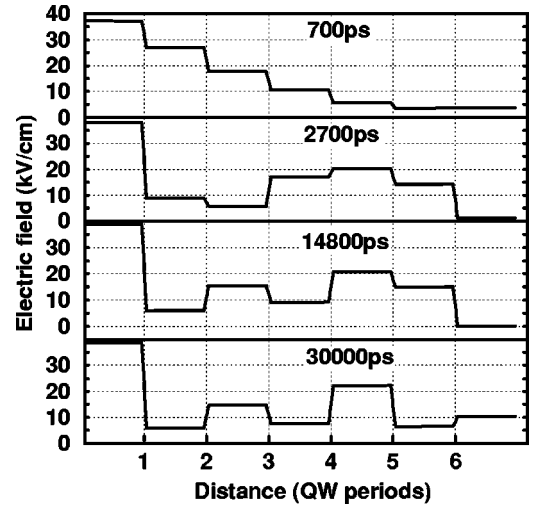


FIG. 3. Spatial electric-field distributions in structure with six QW's at different moments ($E=15$ kV/cm and $I=10^{23}$ cm $^{-2}$ s $^{-1}$).

2). Some of them, for example those corresponding to relatively low and relatively high average electric fields, are less pronounced or have a longer period (compare plots in Fig. 2). In particular, the electric-field distribution in a QW structure with five times lower QW doping for $E=15$ kV/cm [see Fig. 2(d)] is nearly uniform in the QW structure bulk. The features of obtained electric-field spatial distributions can be attributed to the interaction of recharging waves with a short ($\lambda=2L$) and relatively long ($\lambda \leq W$) lengths.

The electric-field distributions and the final state in a QW structure with $N=6$ shown in Fig. 3 reveal the behavior different from that for $N=5$. This implies that in structures with moderate numbers of QW's, the character of the electric-field domains may depend on whether the number of QW's is odd or even.

The excitation of recharging wave with the formation of a stable periodic electric-field domain structure having the period of $\lambda=2L$ in the case of 21 QW's is shown in Fig. 4. The excitation of similar waves and the formation of short-period electric-field distributions were also noted in a struc-

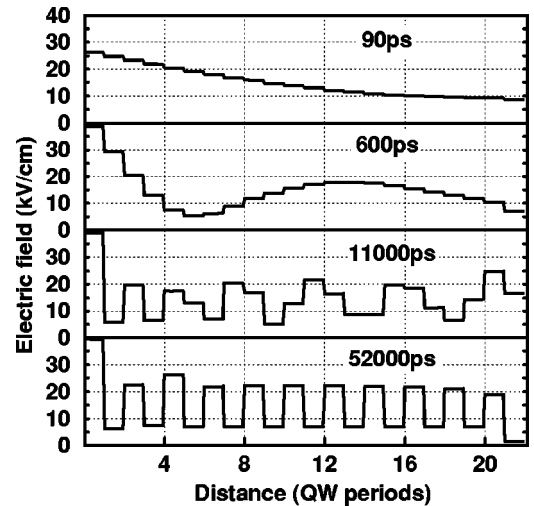


FIG. 4. Evolution of electric-field distribution in QW structure with $N=21$ at $E=15$ kV/cm and $I=10^{23}$ cm $^{-2}$ s $^{-1}$.

ture with 50 QW's. Figure 5 shows the electric-field distributions arisen in a structure with $N=21$ at different average electric fields and intensities. As soon as the amplitudes of recharging waves become high enough, the ordered electric-field domain structures with $\lambda = 2L$ begin to emerge from the emitter side. As shown by our modeling of QW structures with a large number of QW's, the electric-field distributions at relatively early stage of transient processes reveal multiple maxima and minima (the distance between them is longer than the QW structure period L but significantly shorter than the total structure thickness W) moving backwards the electron drift direction. Thus, the phase velocity of the recharging waves excited is directed oppositely to the direction of the electron drift and, hence, the direction of the wave propagation in the case of the Gunn effect. This is in agreement with the theoretical prediction,^{29,30} which is valid for QW structures, at least, for the wave lengths $\lambda \gg L$. A diminished role of the Gunn effect in the cases modeled can be associated with predicted previously¹⁷ a low value of negative differential conductivity in the QW structures in question in comparison to bulk materials as well as with the combination of relatively low-mobile electron concentrations and short distances between contacts.

At not too high intensities, the total photocurrent (created by both the injected and photoexcited electrons) and the mobile electron concentration above the barriers are moderate. Due to the latter, the electron space charge in the barriers is of little importance in determining the electric field. However, at $I \geq 5 \times 10^{23} \text{ cm}^{-2} \text{ s}^{-1}$ the mobile space charge of electrons results in a nonuniformity of the electric field in the barriers. This is seen in Fig. 5(c).

The excitation of waves associated with the QW recharging can be attributed to the decrease of the electron capture rate into a QW when the energy of electrons in some area near that QW increases due to their heating by action of the electric field. Nonlocal character of the electron heating and capture processes gives rise to specific domain structures. The creation of periodic domains specifically with the period equal to twice the QW structure period can be interpreted as follows. Due to the gain of energy by mobile electrons in a barrier with a strong electric field only a small fraction of them can be captured into the following QW. This leads to the decrease in the electron sheet concentration in that QW resulting in its positive charge. As a consequence, the difference in the electric fields in the barriers surrounding the QW increases. Thus, the electric field in the right-hand side barrier becomes lower and this, in turn, leads to a lower energy which electrons gain in the latter barrier and, hence, to a higher capture rate in the next QW. The electric field in the emitter barrier should be relatively high to cause necessary injection current providing the balance between the photoescape and capture of electrons. Hence, the capture probability of electrons strongly heated by the electric field in this barrier is low. This gives rise to the depletion of the first QW and, consequently, other QW's with odd indexes, while even-numbered QW's acquire excessive electrons. As a result, the electric field in odd-numbered barriers is higher than that in even-numbered ones. In QW structures with a period shorter than the electron energy relaxation length, a spatial modulation of the average energy of mobile electrons can be rather weak. In this case, the domain structure can be less

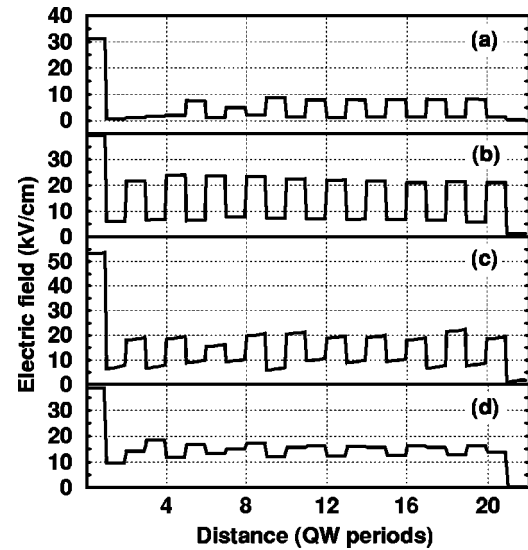


FIG. 5. Stable periodic electric-field domains in QW structure with $N=21$ for (a) $E=5 \text{ kV/cm}$ and $I=10^{23} \text{ cm}^{-2} \text{ s}^{-1}$, (b) $E=15 \text{ kV/cm}$ and $I=10^{23} \text{ cm}^{-2} \text{ s}^{-1}$, (c) $E=15 \text{ kV/cm}$ and $I=10^{24} \text{ cm}^{-2} \text{ s}^{-1}$, and (d) the same as for (b) but with shorter period ($L=34 \text{ nm}$).

pronounced [see the curve for $L=34 \text{ nm}$ in Fig. 5(d)].

Figures 6 and 7 show the transient photocurrents in structures with different number of QW's and at different intensities. The transient photocurrents exhibit the following common features. At the initial stage that takes about one picosecond, the charges of QW's change insufficiently to cause the injection of extra electrons from the emitter contact. After this stage, there is a steep increase in the photocurrent associated with a significant increase of the injected current. The duration of this stage varies over slightly less than two orders of magnitude with changes in the intensity from $I=10^{22}$ to $10^{24} \text{ cm}^{-2} \text{ s}^{-1}$. However, it is virtually independent of the number of QW's. At the next stage, the photocurrent becomes oscillatory. This stage lasts more than 10 ns in all cases studied followed by the stabilization of the photocurrent. The establishment of the photocurrent corresponds to the formation of stable domain structures. It is seen from

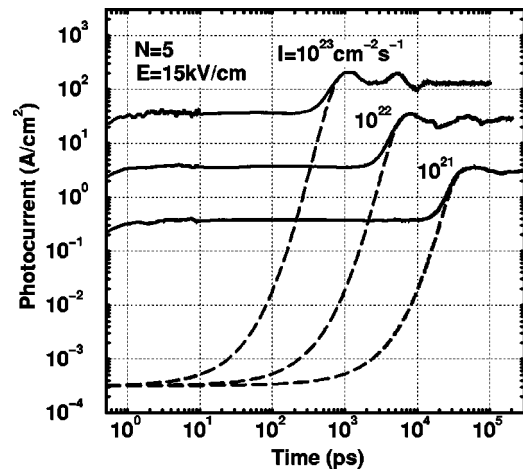


FIG. 6. Densities of transient photocurrent in QW structure with five QW's for different intensities of radiation ($E=15 \text{ kV/cm}$). Injection current densities are shown by dashed lines.

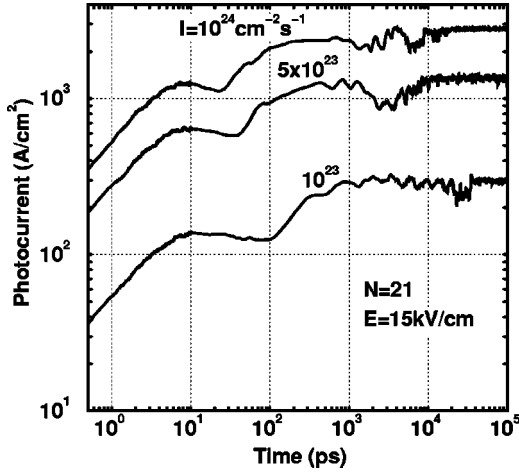


FIG. 7. Densities of transient photocurrent in QW structure with 21 QW's for different intensities of radiation ($E=15$ kV/cm).

Figs. 1, 3, 4, 6, and 7 that the establishment of the steady-state distributions and photocurrents requires different times depending on the number of QW's and the photon flux. In QW structures with $N=5$ and 21 at $E=15$ kV/cm and $I=10^{23}$ $\text{cm}^{-2} \text{s}^{-1}$ the stabilization times are of about 15 and 50 ns, respectively. The revealed features of the transient photocurrent in QW structures are similar to those exhibited by structures on the base on compensated semiconductors.²⁹ The transient photocurrent also resembles (except the oscillatory stage) that in QW structures at low intensities studied previously using a drift-diffusion model.³²

The temporal evolution of the electron system in the QW structures under consideration due to the recharging of QW's can be assessed by the following characteristic times:

$$\tau = \frac{1}{\sigma I}, \quad \tau_c = \frac{L}{p_c v_d}, \quad \text{and} \quad \tau_r = \frac{\omega}{4\pi p_c \sigma_e}. \quad (5)$$

Here, τ is the effective time of the QW emptying due to the photoescape of electrons, τ_c is the capture time, τ_r is the characteristic QW recharging time, p_c is the macroscopic capture parameter (capture probability) related to the QW capture velocity³² v_w by the formula $p_c = v_w / v_d$, v_d is the electron drift velocity in the direction perpendicular to the QW plane, $\sigma_e = (dj_e/dE)|_{E=E_e}$ is the differential conductivity of the emitter contact, and E_e is the electric field at the contact (in the first barrier). For the typical QW structure parameters assumed for the calculation $E=15$ kV/cm and $I=10^{23}$ $\text{cm}^{-2} \text{s}^{-1}$, using the results of our modeling, we obtain the following estimates for the characteristic times given by Eq. (5): $\tau=5$ ns, $\tau_c \approx 5$ ps, and $\tau_r \approx 160$ ps, hence, $\tau/\tau_c \approx 1000$ and $\tau/\tau_r \approx 30$. As it was pointed out above, the capture rate in QW structures with periodic electric-field domains is higher than in those with nearly uniform electric field. Hence, the capture time in such structures should be longer than the estimated value. The electron transit time for QW structures with $N=5-50$ falls in the range of 3–30 ps. Thus, in this case, the QW emptying and recharging times are much longer than other characteristic times. Comparing the transient total and injection photocurrents in Fig. 6, one may conclude that the transition from a low photocurrent at the initial stage to the photocurrent on

the order of its steady-state value is characterized primarily by the recharging time τ_r (see also below), responsible for the redistribution of the potential and the formation of the emitter electric field.

It is of interest, that the values of the steady-state photocurrent in QW structures with the electric-field domains are lower than those calculated for QW structures with nearly neutral bulk. Indeed, the photocurrent density in a QW structure with quasineutral bulk and, hence, uniform electric field in the main part of the structure, is given by the following formula:³³

$$j = e\sigma \Sigma_d I N g \approx \frac{e\sigma \Sigma_d I}{p_c}, \quad (6)$$

where $g \approx (N p_c)^{-1}$ is the photoelectric gain. In this case, the capture parameter is determined by the average electric field mainly via the electric-field dependence of the fraction of electrons having low-enough energy to be captured. Using the calculated data¹⁷ for p_c consistent with experimental results ($p_c=0.06-0.07$), we obtain for the photocurrent density in a 21 QW structure with nearly uniform electric field in its bulk at $E=15$ kV/cm and $I=10^{23}$ $\text{cm}^{-2} \text{s}^{-1}$ the following estimate: $j \approx 457-533$ A/cm². These values exceeds that for a QW structure with a pronounced periodic electric-field domain by the factor of about 1.5 - 1.8. This can be explained by a significant difference in the total capture rate in QW structures with uniform and strongly oscillating electric-field distributions, especially, taking into account nearly exponential drop of the capture rate as a function of the local electric field.^{17,22} Thus, for a rough estimate one can substitute p_c in Eq. (5), corresponding to the electric field equal to the average electric field, by $\langle p_c \rangle$ averaged over the electric field spatial variations. In such a case, the ratio of the photocurrents in a QW structure with nearly uniform electric field and in a QW structure with a pronounced domain structure for the same average electric field can be estimated as $\langle p_c \rangle / p_c$. A distinction between p_c and $\langle p_c \rangle$ originates from the difference in average energies of electrons in these two situations.

Approximating the dependence of p_c on the local electric field \mathcal{E} in the form^{17,22} $p_c \approx \exp(-\mathcal{E}/E_c)$, and assuming that the electric fields in odd- and even-numbered barriers are $\mathcal{E}_{max} = E + \Delta\mathcal{E}/2$ and $\mathcal{E}_{min} = E - \Delta\mathcal{E}/2$, respectively, we obtain

$$\frac{\langle p_c \rangle}{p_c} \approx \cosh\left(\frac{\Delta\mathcal{E}}{2E_c}\right). \quad (7)$$

The notations E_c and $\Delta\mathcal{E}$ denote the characteristic ‘‘capture field’’ and the span of the electric field variations in a domain structure. This explanation is supported by the difference in the average energy of electrons in QW structures with and without domains found in our MC calculations. For the characteristic capture field one may use the following estimate taken from the MC calculations¹⁷ and extracted from the data obtained experimentally:³⁴⁻³⁶ $E_c \approx 6.5-7.5$ kV/cm. For the case $E=15$ kV/cm and $I=10^{23}$ $\text{cm}^{-2} \text{s}^{-1}$, from Fig. 5(b) we can obtain $\Delta\mathcal{E} \approx 15$ kV/cm. Substituting these data into Eq. (7), we obtain $\langle p_c \rangle / p_c \approx 1.5-1.8$ in excellent agreement with the above estimate for the ratio of the photocurrents without and with periodic domain structures.

The dark current and photocurrent in QW structures without the domains under consideration are nearly insensitive to the number of QW's.^{31,37} This is seen from the right-hand side of Eq. (5). A dependence of the current on the number of QW both in dark conditions and under illumination arises due to the contact and charge effects.^{20,22} This dependence is weak when the number of QW's is large enough. However, comparing the densities of steady-state photocurrents for $N = 5$ and 21 in Figs. 6 and 7, we see marked distinctions ($j \approx 130$ and 300 A/cm^2 , respectively). The difference in the photocurrents for structures with $N=5$ and 6 is also impressive (their ratio is approximately of 0.5). The later is attributed to fairly different electric-field distributions in these structures (compare Figs. 1 and 3).

Using Eqs. (3), (5), and (6), τ_r can be estimated as

$$\tau_r \approx \frac{\alpha E_e^2}{4\pi e \sigma \Sigma_d E_t I}.$$

For the emitter electric field one can obtain the estimate^{20,22}

$$E_e \approx \frac{E_t}{\ln(I_m/I)},$$

where

$$I_m = \frac{j_m \langle P_c \rangle}{e \sigma \Sigma_d}.$$

As a result, we obtain

$$\tau_r \approx \frac{\alpha E_t}{4\pi e \sigma \Sigma_d I \ln^2(I_m/I)} \propto \frac{1}{I \ln^2(I_m/I)}. \quad (8)$$

According to Eq. (8), the recharging time τ_r decreases with increasing I slower than I^{-1} . This corresponds to the results shown in Figs. 6 and 7.

The formation of periodic electric-field domains causes periodic distributions of the charges in QW's. This results in the depletion and enrichment of QW's by electrons. In structures with relatively high-characteristic tunneling electric field ($E_t = 340 \text{ kV/cm}$ in our calculations), periodic domains correspond to the depleted odd and enriched even QW's. The occupancies of QW's by electrons (Σ_n/Σ_d) in a structure with $N=21$ are shown in Fig. 8. It is seen that the variations of the electron sheet concentrations in QW's can be of the same order of magnitude as the donor concentration.

IV. DISCUSSION

The phonon mechanism of electron capture into QW's was assumed in the MC model implemented. The electron capture due to electro-electron scattering, at sufficiently high-electron sheet concentrations (in heavily doped QW's), can be nearly as important as that due to polar optical phonon emission.^{38,39} However, such a mechanism also corresponds to a strongly decreasing probability of the capture with increasing electron energy. Hence, the inclusion of the electro-electron capture mechanism should not lead to an essential change in the obtained results.

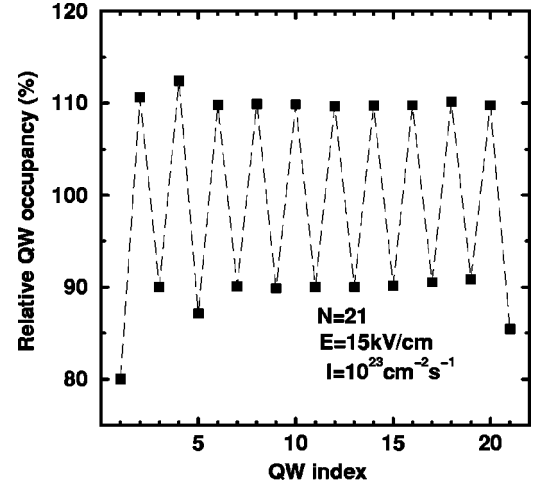


FIG. 8. Occupancies of QW's by electrons (squares) in QW structure with $N=21$ at the same average electric field and intensity as for Fig. 4. Squares are connected by dashed line to emphasize oscillatory nature of electron charge distribution.

Peculiar features of the QW recharging processes in the structures with periodic electric-field domains can manifest themselves in the QW structure frequency-dependent impedance at the frequencies commensurate with the reciprocals of the characteristic times τ , τ_c , and τ_r (see for comparison Refs. 31 and 40). The interchange of the regions with high- and low-electric fields affects the electron dynamics in optically excited QW structures and devices on their base. In particular, this can be actual for QW heterodyne infrared detectors and mixers^{41,42} (see also Ref. 21) as well as for the generation of terahertz radiation in QW structures.^{18,19}

We would like to point out some aspects, which were not clarified above. First of all, this is the question whether periodic electric-field domains with the period equal to twice the QW structure period can arise at much lower excitation powers and in dark conditions. In such situations, the characteristic times of transient processes can be in the microsecond range. Indeed, when $I = 10^{19} - 10^{20} \text{ cm}^{-2} \text{ s}^{-1}$, one obtains $\tau = 0.5 - 5 \mu\text{s}$. However, the study of prolonged transient processes (say, in the microsecond range) in the structures in question by ensemble MC particle methods is, unfortunately, complicated due to an inherent drawback of such calculation techniques—excessively long computation time. Drift-diffusion models of electron transport in QW structures similar to that used previously,^{11,13,32} valid for an overall assessment of such structures, cannot be applied in our case. This is due to the importance of nonequilibrium electron processes when the characteristic dimensions (such as the QW structure period) commensurate with the electron energy relaxation length, i.e., when the effects of nonlocality are crucial. Possibly, the problem of periodic electric-field domains at low intensities and in dark conditions can be effectively resolved using a hydrodynamic electron-transport model (for example, see Refs. 43–45 and references therein), generalized by the inclusion of the QW recharging effects. Another question is concerned with the possibility of the undamped photocurrent oscillations due to either the recharging waves³⁸ or the Gunn effect complicated by the recharging processes.¹⁶ It requires, however, a separate study.

V. CONCLUSION

We studied transient processes and formation of periodic electric-field domains in multiple QW structures excited by infrared radiation triggering electron bound-to-continuum transitions. An ensemble MC particle method was used to

calculate the electric-field and charge distributions and the transient photocurrents. The origin of periodic electric-field domains is associated with the excitation of recharging waves due to decreasing capture rate of electrons with their heating by the electric field.

*Electronic address: v-ryzhii@u-aizu.ac.jp

- ¹L. Esaki and R. Tsu, *IBM J. Res. Dev.* **14**, 61 (1970).
- ²R. Tsu and L. Esaki, *Appl. Phys. Lett.* **19**, 246 (1971).
- ³S.H. Kwok, H.G. Grahn, M. Ramsteiner, K. Ploog, F. Prengel, A. Wacker, E. Schoöll, S. Murugar, and R. Merlin, *Phys. Rev. B* **51**, 9943 (1995).
- ⁴A. Wacker, M. Moscoso, M. Kindelan, and L.L. Bonilla, *Phys. Rev. B* **55**, 2466 (1997).
- ⁵M. Morifujii and C. Hamaguchi, *Phys. Rev. B* **58**, 12 842 (1998).
- ⁶M. Helm, W. Hilber, G. Strasser, R. De Meester, F.M. Peeters, and A. Wacker, *Phys. Rev. Lett.* **82**, 3120 (1999).
- ⁷J. Faist, F. Capasso, D.L. Sivco, C. Sirtori, A.L. Hutchinson, and A.Y. Chou, *Science* **264**, 553 (1994).
- ⁸E. Schomburg, T. Blomeier, K. Hofbeck, J. Grenzer, S. Brandl, I. Lingott, A.A. Ignatov, and K.F. Renk, *Phys. Rev. B* **58**, 4035 (1998).
- ⁹A.A. Ignatov and A.-P. Jauho, *J. Appl. Phys.* **85**, 3643 (1999).
- ¹⁰B.F. Levine, *J. Appl. Phys.* **74**, R1 (1993).
- ¹¹S.R. Andrews and B.A. Miller, *J. Appl. Phys.* **70**, 993 (1991).
- ¹²M. Ershov, V. Ryzhii, and C. Hamaguchi, *Appl. Phys. Lett.* **67**, 3147 (1995).
- ¹³L. Thibaudeau, P. Bois, and J.Y. Duboz, *J. Appl. Phys.* **79**, 446 (1996).
- ¹⁴M. Ershov, H.C. Liu, Z.R. Wasilewski, M. Buchanan, and V. Ryzhii, *Appl. Phys. Lett.* **70**, 414 (1997).
- ¹⁵A. Sa'ar, C. Mermelstein, H. Schneider, C. Schoenbein, and M. Walther, *IEEE Photonics Technol. Lett.* **10**, 1470 (1998).
- ¹⁶N. Schneider, C. Mermelstein, R. Rehm, C. Schönbein, A. Sa'ar, and M. Walther, *Phys. Rev. B* **57**, R15 096 (1998).
- ¹⁷M. Ryzhii and V. Ryzhii, *Jpn. J. Appl. Phys., Part 1* **38**, 5922 (1999).
- ¹⁸M. Ryzhii and V. Ryzhii, *Appl. Phys. Lett.* **72**, 842 (1997).
- ¹⁹M. Ryzhii, V. Ryzhii, and M. Willander, *J. Appl. Phys.* **84**, 3403 (1998).
- ²⁰V. Ryzhii, *J. Appl. Phys.* **81**, 6442 (1997).
- ²¹V. Ryzhii, I. Khmyrova, and M. Ryzhii, *Jpn. J. Appl. Phys., Part 1* **36**, 2596 (1997).
- ²²V. Ryzhii and H.C. Liu, *Jpn. J. Appl. Phys., Part 1* **38**, 5815 (1999).
- ²³J.A. Brum and G. Bastard, *Phys. Rev. B* **33**, 1420 (1986).
- ²⁴P.W.M. Blom, C. Smit, J.E.M. Haverkort, and J.H. Wolter, *Phys. Rev. B* **47**, 2072 (1993).
- ²⁵D. Morris, D. Deveaud, A. Regreny, and P. Auvray, *Phys. Rev. B* **47**, 6819 (1993).
- ²⁶J.M. Gerard, B. Deveaud, and A. Regreny, *Appl. Phys. Lett.* **63**, 240 (1993).
- ²⁷A. Zakharova and V. Ryzhii, *Fiz. Tekh. Poluprovodn.* **25**, 402 (1991) [*Sov. Phys. Semicond.* **25**, 244 (1991)].
- ²⁸L.F. Register and K. Hess, *Appl. Phys. Lett.* **71**, 1222 (1997).
- ²⁹R.F. Kazarinov, R.A. Suris, and B.I. Fuks, *Fiz. Tekh. Poluprovodn.* **7**, 149 (1973) [*Sov. Phys. Semicond.* **7**, 102 (1973)].
- ³⁰R.A. Suris and B.I. Fuks, *Fiz. Tekh. Poluprovodn.* **7**, 1556 (1973) [*Sov. Phys. Semicond.* **7**, 1039 (1973)].
- ³¹R.A. Suris and B.I. Fuks, *Fiz. Tekh. Poluprovodn.* **4**, 1507 (1980) [*Sov. Phys. Semicond.* **14**, 896 (1980)].
- ³²M. Ershov, C. Hamaguchi, and V. Ryzhii, *Jpn. J. Appl. Phys., Part 1* **35**, 1395 (1996).
- ³³H.C. Liu, *Appl. Phys. Lett.* **60**, 1507 (1992).
- ³⁴E. Rosencher, B. Vinter, F. Luc, L. Thibaudeau, P. Bois, and J. Nagle, *IEEE J. Quantum Electron.* **30**, 2875 (1994).
- ³⁵H.C. Liu, M. Buchanan, and Z.R. Wasilewski, *J. Appl. Phys.* **82**, 889 (1997).
- ³⁶J.-C. Chang, S.S. Li, M.Z. Tidrow, P. Ho, M. Tsai, and C.P. Lee, *Appl. Phys. Lett.* **69**, 2412 (1996).
- ³⁷A.G. Steele, H.C. Liu, M. Buchanan, and Z.R. Wasilewski, *J. Appl. Phys.* **72**, 1062 (1992).
- ³⁸P. Sotileris and K. Hess, *Phys. Rev. B* **49**, 7543 (1994).
- ³⁹K. Kalna, M. Mosko, and F.M. Peeters, *Appl. Phys. Lett.* **68**, 117 (1996).
- ⁴⁰R.A. Suris and B.I. Fuks, *Fiz. Tekh. Poluprovodn.* **9**, 1717 (1975) [*Sov. Phys. Semicond.* **9**, 1130 (1975)].
- ⁴¹E. Brown, K.A. McIntosh, F.W. Smoth, and M.J. Manfra, *Appl. Phys. Lett.* **62**, 1513 (1993).
- ⁴²H.C. Liu, J. Li, E.R. Brown, K.A. McIntosh, K.B. Nichols, and M.J. Manfra, *IEEE J. Quantum Electron.* **32**, 1024 (1996).
- ⁴³R. Stratton, *Phys. Rev.* **126**, 2002 (1962).
- ⁴⁴P.A. Sandborn, A. Rao, and P.A. Blakey, *IEEE Trans. Electron Devices* **36**, 1244 (1989).
- ⁴⁵D.L. Woolard, H. Tian, M.A. Littlejohn, and K.W. Kim, *Phys. Rev. B* **44**, 11 119 (1991).